Research Square

Preprints are preliminary reports that have not undergone peer review.
They should not be considered conclusive, used to inform clinical practice,
or referenced by the media as validated information.

Deciphering the Binding Mechanism of PSMA-1007 to PSMA: Insights from Molecular Dynamics and Free Energy Landscapes

Weiqiang Huang
The Second Affiliated Hospital of Guangxi Medical University
Futian Hu
The Second Affiliated Hospital of Guangxi Medical University
Xi Cao
The Second Affiliated Hospital of Guangxi Medical University
Yiming Wei
The Second Affiliated Hospital of Guangxi Medical University
Mingju Zheng
The Second Affiliated Hospital of Guangxi Medical University
Zonglin Li
The Second Affiliated Hospital of Guangxi Medical University
Zheng Zhao
The Second Affiliated Hospital of Guangxi Medical University
Wenjie Liu
The Second Affiliated Hospital of Guangxi Medical University
Xia Li
The Second Affiliated Hospital of Guangxi Medical University
Shidong Lian
bookinsect@126.com

The Second Affiliated Hospital of Guangxi Medical University

Article

Keywords: PSMA inhibitor, Binding energy, Molecular dynamics, Prostate cancer

Posted Date: February 27th, 2026

DOI: https://doi.org/10.21203/rs.3.rs-8866982/v1

License: This work is licensed under a Creative Commons Attribution 4.0 International License.
Read Full License

Additional Declarations: No competing interests reported.

Abstract

This study aimed to investigate the targeted binding mechanism of PSMA-1007 to prostate-specific membrane antigen (PSMA) at the atomic level, providing a theoretical basis for the rational design of PSMA-targeted drugs. We employed molecular dynamics (MD) simulations combined with the MM/PBSA (Molecular Mechanics Poisson-Boltzmann Surface Area) free energy calculation method. The results revealed a strong binding affinity with a total binding free energy of -75 kcal/mol, which was primarily driven by favorable electrostatic interactions. The stability of the complex was further supported by the persistent formation of a substantial number of hydrogen bonds (5 to 14) between PSMA-1007 and PSMA throughout the simulation. Free energy decomposition analysis identified key hotspot residues, including LYS699, ARG463, and TYR700, which made significant contributions to the binding. Quantitative assessment of the two major binding pockets showed that the S1 and S1' pockets contributed approximately 20% and 40% of the total favorable binding energy, respectively, highlighting the critical role and specificity of these subsites. In conclusion, our findings elucidate the dynamic binding process and energetic landscape of PSMA-1007, offering valuable insights for structure-based drug design targeting PSMA.

Introduction

Prostate cancer is one of the most commonly diagnosed malignancies among men worldwide, and its accurate diagnosis and effective treatment remain major clinical challenges [1, 2]. Prostate-specific membrane antigen (PSMA), a type II transmembrane glycoprotein, is highly overexpressed on the surface of prostate cancer cells—particularly in advanced, castration-resistant, and metastatic lesions—making PSMA one of the most promising targets for theranostic applications in prostate cancer management [3, 4]. The extracellular domain of PSMA exhibits glutamate carboxypeptidase activity, and its catalytic pocket serves as an ideal site for designing small-molecule inhibitors with high affinity and specificity [5].

Against this background, PSMA-targeted radiopharmaceuticals have achieved revolutionary progress[6]. Compared with earlier compounds such as PSMA-617, PSMA-1007 possesses unique pharmacokinetic properties, especially low hepatobiliary excretion, which significantly reduces urinary interference in the pelvic region and thereby enhances detection of local recurrence and metastatic lesions in prostate cancer [7].

Although the radiopharmaceutical PSMA-1007 has been widely adopted in clinical settings worldwide and its high targeting efficiency has been well validated, its dynamic binding process with PSMA at the atomic level remains incompletely understood. Specifically, the formation and stability of key interactions, as well as the underlying energetics of the binding process, have yet to be fully elucidated. Current understanding of the specific interaction between PSMA-1007 and PSMA primarily relies on static “snapshots” derived from the co-crystal structures of its analogs (e.g., PSMA-617) with PSMA [8]. However, protein–ligand binding is a highly dynamic and complex process, in which static structures fail

to capture conformational transitions, intermediate states, and transient interactions involving key residues. Molecular dynamics (MD) simulation is a powerful computational tool that complements experimental techniques by modeling the time-resolved motions of biomolecules at atomic resolution. It provides a dynamic perspective on drug–target interactions, enabling exploration of binding free energy landscapes, identification of “hotspot” residues, and visualization of binding pathways. These insights offer valuable guidance for the rational design and optimization of next-generation ligands.

This study aims to employ molecular dynamics simulationsto systematically investigate the binding mechanism between PSMA-1007 and PSMA. By offering a comprehensive molecular-level understanding of this interaction, our work will lay a solid theoretical foundation for the development of novel PSMA-targeted agents with improved pharmacokinetic properties.

Materials and Methods

The structural model used in this study was derived from the X-ray crystal structure of human glutamate carboxypeptidase II (GCPII) in complex with the urea-based inhibitor PSMA-1007 [9, 10], with a reported resolution of 1.43 Å for PSMA. Molecular dynamics (MD) simulations were performed using the GROMACS 2023.2 software package [11]. The protein–ligand complex was prepared using the Solution Builder module in CHARMM-GUI. A solvent box was constructed with a minimum distance of 10 Å from the complex to the box edge, and the system was solvated with TIP3P water molecules, along with sodium and chloride ions to neutralize the overall charge and maintain an ionic concentration of 0.15 mol/L.

The system temperature was set to 310.15 K, and periodic boundary conditions were applied. Grid information for PME-FFT was automatically generated, and the CHARMM36m force field parameters were applied to all atoms to generate the topology file [12–15]. Energy minimization was carried out using the steepest descent algorithm for up to 5000 steps. The particle mesh Ewald (PME) method was employed to calculate long-range electrostatic interactions. The minimization process was terminated when the maximum force on all atoms was less than 1000 $kJ \cdot mol^{-1} \cdot nm^{-1}$. Following energy minimization, a 125-ps pre-equilibration was performed under an NPT ensemble at constant pressure and temperature, with a controlled heating rate. The final MD production run lasted for 100 ns with a 2-fs time step. Once the system reached equilibrium, the molecular mechanics Poisson–Boltzmann surface area (MM-PBSA) method was used to calculate the binding free energy between the protein and ligand using gmx_MMPBSA [16, 17].

Results and Discussion

As shown in Fig. 1(a), we first explored the stability of the PSMA-1007 and PSMA complex by analyzing the Root Mean Square Deviation (RMSD) of the complex. The RMSD of PSMA stabilized at approximately 58 ns (Fig. 1(a), 0.255514 ± 0.054228 nm), indicating that thereafter, there were no significant fluctuations, which suggests that the structure of PSMA remains in an energetically stable state. In

contrast, the RMSD of PSMA-1007 quickly maintained a small fluctuation shortly after the initiation of the simulation, indicating that the frequency of reversible covalent bonding has led PSMA-1007 to reach an energetically saturated state Moreover, the difference between the maximum and minimum values of PSMA-1007's RMSD (ΔRMSD) is < 0.2 nm, suggesting that the conformational changes of PSMA-1007 are minimal, and significant torsional movements of the covalent bond do not occur [19][20].

To further understand the binding process, we analyzed the Root Mean Square Fluctuation (RMSF) of the complex, providing insights into the displacement of amino acids during the simulation (Fig. 1(b)). Amino acid residues near the N-terminus and C-terminus (i.e., at the ends or breakpoints) exhibited greater fluctuations. This increased fluctuation is attributed to these regions' inability to form stable covalent bonds and their frequent contact with water molecules, as well as the inherently flexible nature of the residues in these regions [21]. In contrast, the RMSF values around amino acid residues 70–110, 352–486, 523, and 588 displayed significantly smaller fluctuations compared to other regions, indicating that the conformations of these residues do not undergo flexible changes and remain in a relatively stable state. On the other hand, the regions with higher RMSF fluctuations indicate that amino acid residues may frequently engage in non-covalent interactions with other secondary structures and PSMA-1007, suggesting that these areas may represent more flexible binding sites [22].

Figure 1(c), illustrates the overall radius of gyration (RG) of PSMA during the simulation process (RG = 2.625849 ± 0.025465 nm). Although there are slight fluctuations in the RG values, the variations remain within a range of less than 0.2 nm (ΔRG < 0.2 nm), indicating that while PSMA maintains the stability of its overall structure, there may be anisotropic local conformational adjustments occurring. However, the impact of these adjustments on the spatial dimensions of the overall conformation is minimal [23][24]. This phenomenon suggests that PSMA may achieve its biological functions through a structural design that is regulated by both rigid and flexible regions; the rigid core maintains structural integrity, while directionally selective flexibility allows for necessary conformational adjustments. These dynamic characteristics might play a crucial role in molecular recognition or signal transduction processes.

The Solvent-Accessible Surface Area (SASA) is an important concept in structural biology and biochemistry, used to describe the area of a biomolecule's surface (such as proteins and nucleic acids) that is accessible to solvent molecules [25, 26]. As depicted in Fig. 1(d), we observe that SASA reaches its maximum after 58 ns during the simulation, followed by no significant fluctuations. This observation is consistent with the results of the RMSD analysis, indicating that its quaternary structure undergoes sufficient relaxation thereafter, maintaining energy stability.

The number of hydrogen bonds is a critical parameter for maintaining the relative positions between molecules and represents one of the most common and readily formed non-covalent interactions [27]. Previous indicators have shown that the complex reaches a relatively stable state after approximately 58 ns. Therefore, we analyzed the formation of hydrogen bonds between PSMA-1007 and PSMA during the 40–100 ns simulation period (Fig. 2). The results revealed that up to14 hydrogen bonds could be formed, with the number generally fluctuating within the range of 5 to 14 throughout the simulation. In addition to

classical hydrogen bonds, short-range polar interactions within 0.35 nm—though not classified as hydrogen bonds by GROMACS—also contribute significantly to the stability of the complex [28]. These interactions were observed to reach a maximum of 17, and generally remained within the range of 4 to 17, which is highly favorable for maintaining the stable binding between the protein and the small-molecule ligand [29, 30].

To evaluate the receptor–ligand binding efficacy from an energetic perspective, we calculated the target-binding free energy of PSMA-1007 using the Molecular Mechanics Poisson–Boltzmann Surface Area (MM-PBSA) method [31]. Through MM-PBSA analysis, we found that the total binding free energy was −75 kcal/mol, indicating strong targeting capability of PSMA-1007. This result theoretically supports previous reports [32]. Additionally, we investigated the contribution of residues within 4 Å of the ligand to binding, as these are crucial for drug optimization and mechanistic understanding. Based on their contributions to the binding energy, we generated a corresponding hotspot map (Fig. 3), where blue regions indicate favorable contributions and red regions represent unfavorable contributions. From Fig. 3, we observe that the green-colored PSMA-1007 molecular structure is enclosed within a predominantly blue binding pocket, with some red portions present—indicating that PSMA-1007 is tightly bound within the PSMA binding pocket.

According to previous reports, PSMA has two binding pockets for urea-based inhibitors. One is the S1' pocket, known as the “glutarate sensor,” composed of side chains from amino acid residues Gly427, Gly518, Phe209, Asn257, Leu428, Lys699, and Tyr700. The amino acid residues Lys699 and Tyr700 specifically bind to the glutamate portion of the NAAG structure and are critical for catalyzing the deglutamylation process. The other recognition site is the S1 pocket, which contains the “arginine patch” formed by Arg463, Arg534, and Arg536 [33–36]. However, the exact energetic contributions of the S1 and S1' pockets remained unquantified until this study. Figure 4 illustrates the energy contributions of several key residues—including Lys699, Arg463, and Tyr700—which demonstrated significant favorable interactions. Statistical analysis revealed that the S1 and S1' pockets contributed approximately 20% and 40% of the total favorable binding energy, respectively. This provides a direct and quantitative assessment of binding specificity, offering robust theoretical support for future drug design and optimization.

Conclusion

In this study, we employed molecular dynamics simulations to investigate the targeting binding mechanism of PSMA-1007 at the atomic scale. We elucidated the dynamic process of PSMA-1007 binding with PSMA, identified the key interactions, examined the stability, and provided the energetic foundation for the entire binding process. Through MMPBSA analysis, we found that the total binding free energy was − 75 kcal/mol, which theoretically validates the targeting binding affinity of PSMA-1007. Additionally, we identified the crucial roles of residues such as LYS699, ARG463, and TYR700 in the binding process. Statistical analysis revealed that the contributions of residues in the S1 and S1’ pockets

accounted for 20% and 40% of the favorable contributions, respectively. This provides a clear and scientifically robust demonstration of the binding specificity, offering theoretical support for the development and improvement of subsequent drugs.

Declarations

Data Availability

All data generated or analysed during this study are included in this published article. The raw datasets generated during the current study are available from the corresponding author on reasonable request.

Author Contributions

All authors contributed to the study conception and design. Material preparation, data collection, and analysis were performed by [Weiqiang Huang] and [Shidong Lian]. The first draft of the manuscript was written by [Weiqiang Huang], and all authors commented on previous versions of the manuscript. All authors read and approved the final manuscript.

Funding

The authors declare that no funds, grants, or other support were received during the preparation of this manuscript.

Competing Interests

The author(s) declare no competing interests.

Ethics approval

This study was performed in line with the principles of the Declaration of Helsinki. Approval was granted by the Ethics Committee of the Second Affiliated Hospital of Guangxi Medical University (Date2024/2/27/No 2024-KY□0304□)

References

1. Bosland MC. Prostate Cancer. Carcinogenicity. 2021:715-46.
2. Siegel RL, Miller KD, Wagle NS, Jemal A. Cancer statistics, 2023. CA: A Cancer Journal for Clinicians. 2023;73(1):17-48.
3. Israeli RS, Powell CT, Corr JG, Fair WR, Heston WDW. Expression of the Prostate-specific Membrane Antigen. Cancer Research. 1994;54(7):1807-11.
4. Silver DA, Pellicer I, Fair WR, Heston WD, Cordon-Cardo C. Prostate-specific membrane antigen expression in normal and malignant human tissues. Clinical Cancer Research. 1997;3(1):81-5.

5. Mesters JR, Barinka C, Li W, Tsukamoto T, Majer P, Slusher BS, et al. Structure of glutamate carboxypeptidase II, a drug target in neuronal damage and prostate cancer. Embo Journal. 2014;25(6):1375-84.
6. Giesel FL, Hadaschik B, Cardinale J, Radtke J, Vinsensia M, Lehnert W, et al. F-18 labelled PSMA-1007: biodistribution, radiation dosimetry and histopathological validation of tumor lesions in prostate cancer patients. Eur J Nucl Med Mol Imaging. 2017;44(4):678-88.
7. Rauscher I, Krnke M, Knig M, Gafita A, Maurer T, Horn T, et al. Matched-Pair Comparison of 68Ga-PSMA-11 PET/CT and 18F-PSMA-1007 PET/CT: Frequency of Pitfalls and Detection Efficacy in Biochemical Recurrence After Radical Prostatectomy. The Journal of Nuclear Medicine. 2019;61:51 - 7.
8. Schäfer M, Bauder-Wüst U, Roscher M, Motlová L, Kutilová Z, Remde Y, et al. Structure-Activity Relationships and Biological Insights into PSMA-617 and Its Derivatives with Modified Lipophilic Linker Regions. ACS Omega. 2025;10(7):7077-90.
9. Berman H, Henrick K, Nakamura H. Announcing the worldwide Protein Data Bank. Nature Structural & Molecular Biology. 2003;10(12):980-.
10. Pavlicek J, Ptacek J, Barinka C. Glutamate Carboxypeptidase II: An Overview of Structural Studies and Their Importance for Structure-Based Drug Design and Deciphering the Reaction Mechanism of the Enzyme. Current Medicinal Chemistry. 2012;19(9):-.
11. Abraham MJ, Murtola T, Schulz R, Páll S, Lindahl E. GROMACS: High performance molecular simulations through multi-level parallelism from laptops to supercomputers. Softwarex. 2015;1-2(C):19-25.
12. Essmann U, Perera L, Berkowitz ML, Darden T, Lee H, Pedersen LG. A smooth particle mesh Ewald method. The Journal of Chemical Physics. 1995;103(19):8577-93.
13. Huang J, Rauscher S, Nawrocki G, Ran T, Mackerell AD. CHARMM36m: An Improved Force Field for Folded and Intrinsically Disordered Proteins. Biophysical Journal. 2017;112(3):175a-6a.
14. Jo S, Kim T, Iyer VG, Im W. CHARMM-GUI: A web-based graphical user interface for CHARMM. Journal of Computational Chemistry. 2008;29(11).
15. Jorgensen WL, Chandrasekhar J, Madura JD, Impey RW, Klein ML. Comparison of simple potential functions for simulating liquid water. The Journal of Chemical Physics. 1983;79(2):926-35.
16. Berendsen HJC, Postma JPM, van Gunsteren WF, DiNola A, Haak JR. Molecular dynamics with coupling to an external bath. The Journal of Chemical Physics. 1984;81(8):3684-90.
17. Valdés-Tresanco MS, Valdés-Tresanco ME, Valiente PA, Moreno E. gmx_MMPBSA: A New Tool to Perform End-State Free Energy Calculations with GROMACS. Journal of Chemical Theory and Computation. 2021;17(10):6281-91.
18. Bakan A, Meireles LM, Bahar I. ProDy: Protein Dynamics Inferred from Theory and Experiments. Bioinformatics. 2011;27(11):1575-7.
19. Genheden S, Ryde U. The MM/PBSA and MM/GBSA methods to estimate ligand-binding affinities. Expert Opinion on Drug Discovery. 2015;10(5):449-61.

20. Levi, C. T, Pierce, Romelia, Salomon-Ferrer, Cesar, et al. Routine Access to Millisecond Time Scale Events with Accelerated Molecular Dynamics. Journal of Chemical Theory and Computation. 2012;8(9):2997-3002.
21. Shrivastava IBRLBH. Normal Mode Analysis of Biomolecular Structures: Functional Mechanisms of Membrane Proteins. Chemical Reviews. 2010;110(3).
22. Marcelo CR, Melo, Rafael C, Bernardi, Till, Rudack, et al. NAMD goes quantum: an integrative suite for hybrid simulations. Nature methods. 2018.
23. Kohn JE, Millett IS, Jacob J, Zagrovic B, Dillon TM, Cingel N, et al. Random-coil behavior and the dimensions of chemically unfolded proteins. Proceedings of the National Academy of Sciences of the United States of America. 2004;101(34):12491-6.
24. Dill KA, Ghosh K, Schmit JD. Physical limits of cells and proteomes. Proceedings of the National Academy of Sciences of the United States of America. 2011;108(44):p.17876-82.
25. Marsh JA, Teichmann SA, Forman-Kay JD. Probing the diverse landscape of protein flexibility and binding. Current Opinion in Structural Biology. 2012;22(5).
26. Frank, Eisenhaber, Philip, Lijnzaad, Patrick, Argos, et al. The double cubic lattice method: Efficient approaches to numerical integration of surface area and volume and to dot surface contouring of molecular assemblies. Journal of Computational Chemistry. 1995.
27. Jeffrey GA. An introduction to hydrogen bonding: An introduction to hydrogen bonding; 1997.
28. Baker EN, Hubbard RE. Hydrogen bonding in globular proteins. Progress in Biophysics & Molecular Biology. 1984;44(2):97-179.
29. Kumar S, Nussinov R. Close-range electrostatic interactions in proteins. Chembiochem A European Journal of Chemical Biology. 2015;3(7):604-17.
30. Bissantz C, Kuhn B, Stahl M. A Medicinal Chemist's Guide to Molecular Interactions. Journal of Medicinal Chemistry. 2010.
31. Kollman PA, Massova I, Reyes C, Kuhn B, Iii TEC. Calculating structures and free energies of complex molecules: combining molecular mechanics and continuum models. Cheminform. 2010;32(12):no-no.
32. Schäfer M, Bauder-Wüst U, Leotta K, Zoller F, Mier W, Haberkorn U, et al. A dimerized urea-based inhibitor of the prostate-specific membrane antigen for 68Ga-PET imaging of prostate cancer. EJNMMI Research. 2012;2(1):23.
33. Mease RC, Dusich CL, Foss CA, Ravert HT, Dannals RF, Seidel J, et al. N-[N-[(S)-1,3-Dicarboxypropyl]carbamoyl]-4-[18F]fluorobenzyl-L-cysteine, [18F]DCFBC: A new imaging probe for prostate cancer. Clinical Cancer Research. 2008;14(10):3036-43.
34. Mengxia, Chen, Xuefeng, Qiu, Qing, Zhang, et al. PSMA uptake on [68Ga]-PSMA-11-PET/CT positively corrects with prostate cancer aggressiveness. The quarterly journal of nuclear medicine and molecular imaging : official publication of the Italian Association of Nuclear Medicine (AIMN) [and] the International Association of Radiopharmacology (IAR), [and] Section of the Society of.

35. Maresca KP, Hillier SM, Femia FJ, Keith D, Barone C, Joyal JL, et al. A series of halogenated heterodimeric inhibitors of prostate specific membrane antigen (PSMA) as radiolabeled probes for targeting prostate cancer. Journal of Medicinal Chemistry. 2009;52(2):347-57.

36. □□. Lys-urea-Glu□PET□□□□□□□□□□□□□□□□□□: □□□□□□; 2023.

Figures

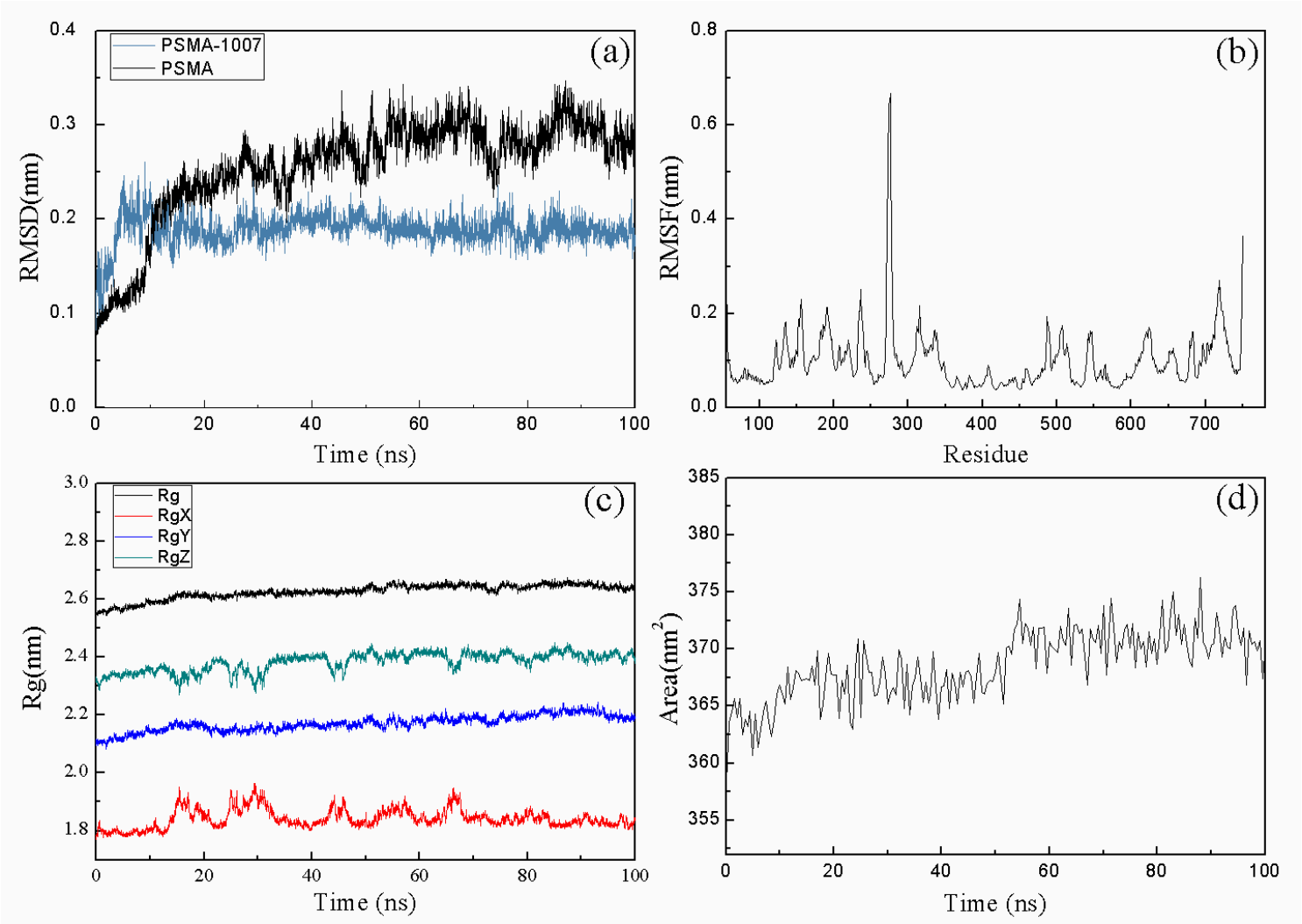


Figure 1

□a□RMSD of PSMA and PSMA-1007□(b) RMSF of PSMA in the complex□(c) Rg of PSMA□(d) SASA of PSMA over the simulation time.

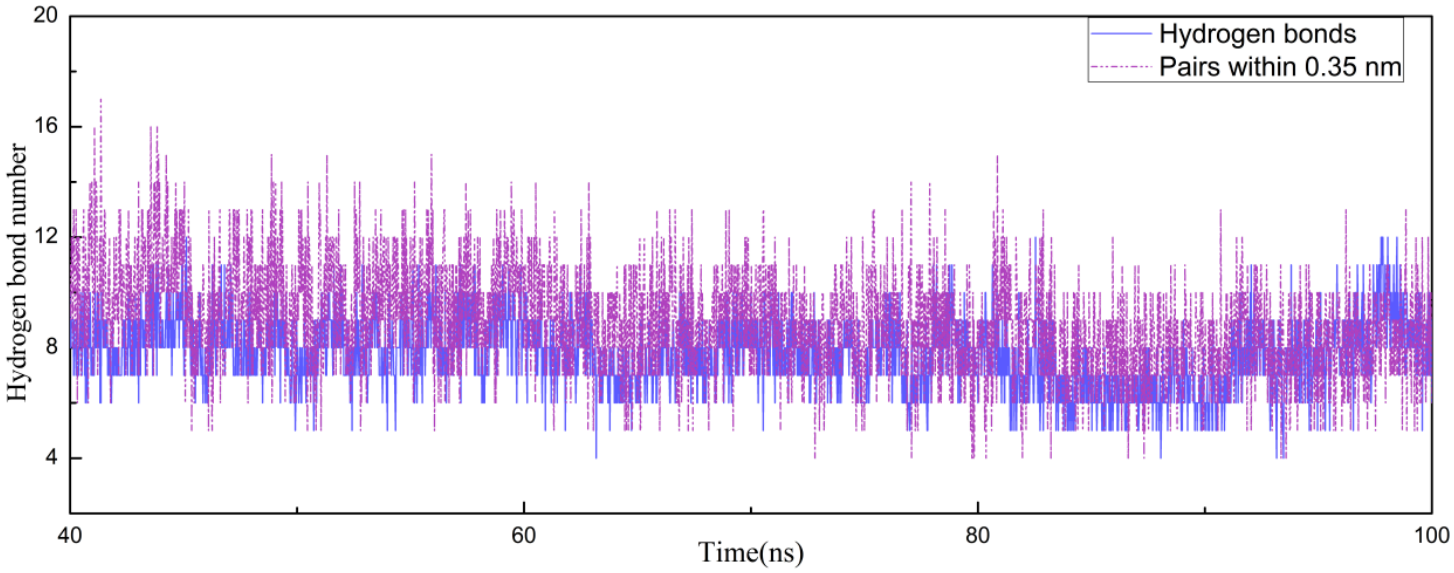


Figure 2

Hydrogen bond generated between protein-ligand.

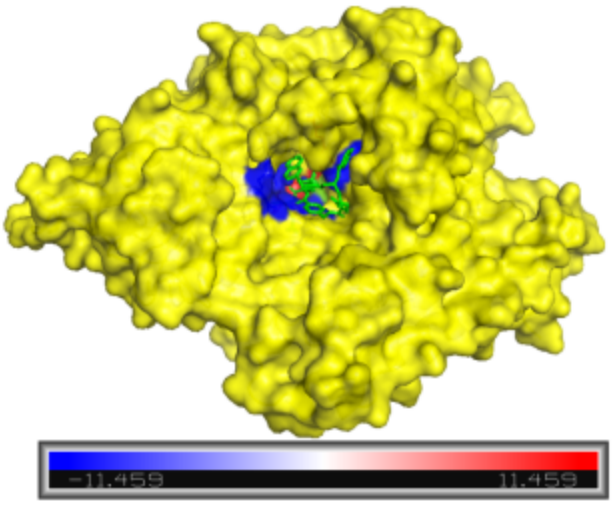


Figure 3

A heat map showing the energy contribution distribution of residues within 4 Å of the ligand. Contributions are color-coded: favorable (blue), unfavorable (red), and PSMA-1007 (green).

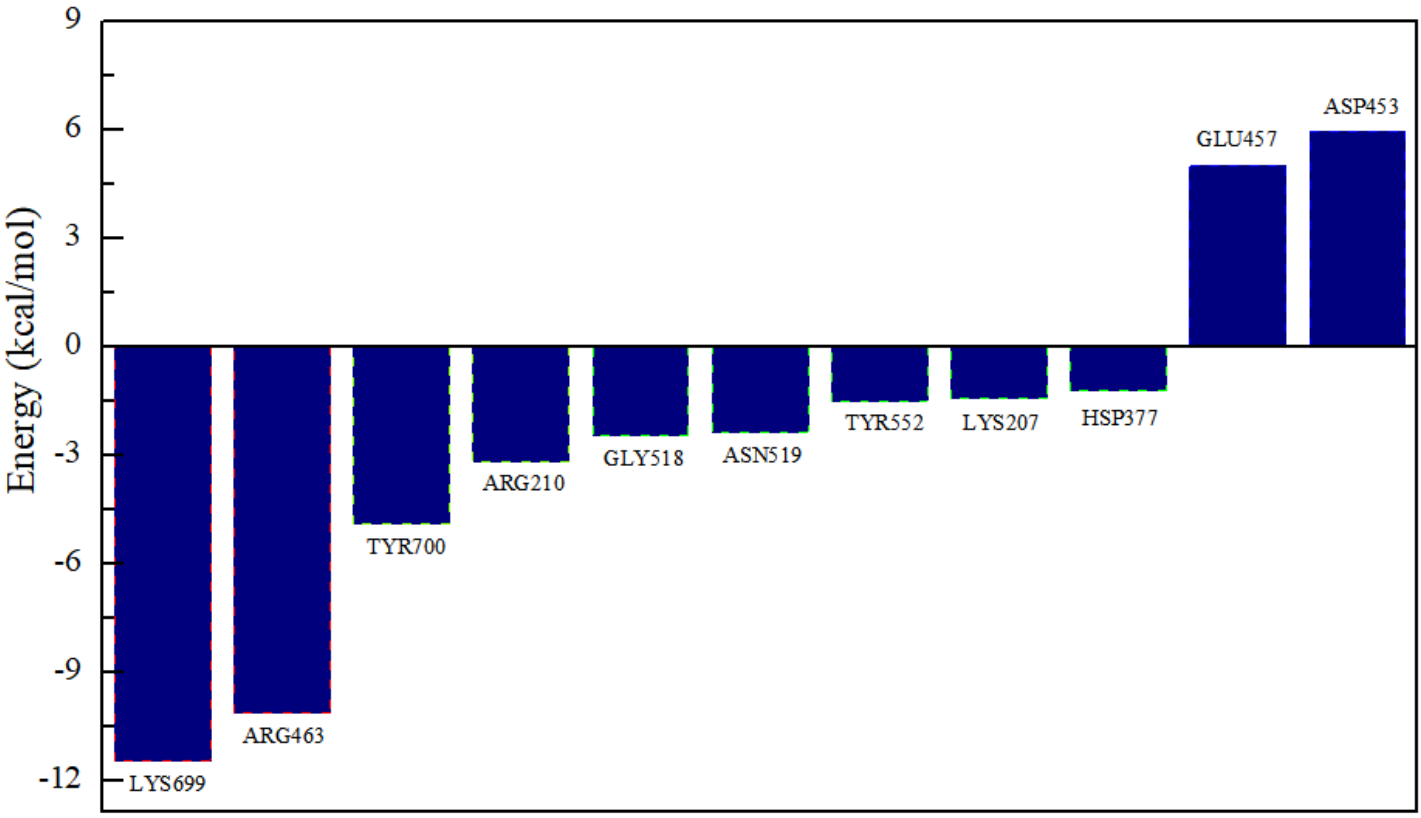


Figure 4

A histogram showing the residues with notable contributions and their corresponding contribution energies.